Quaternary Science Reviews 263 (2021) 106978

Contents lists available at ScienceDirect

Quaternary Science Reviews

journal homepage: www.elsevier.com/locate/quascirev

Opposite dust grain-size patterns in the Pacific and Atlantic sectors of the Southern Ocean during the last 260,000 years

Michèlle van der Does [a, *, 1], Marc Wengler [a, b, 1], Frank Lamy [a, b], Alfredo Martínez-García [c], Samuel L. Jaccard [d, e], Gerhard Kuhn [a, b], Verena Lanny [f], Jan-Berend W. Stuut [g, h], Gisela Winckler [i]

[a] Alfred Wegener Institute, Helmholtz Center for Polar and Marine Research, Department of Marine Geology, Bremerhaven, Germany
[b] MARUM Center for Marine Environmental Sciences, University of Bremen, Bremen, Germany
[c] Max Planck Institute for Chemistry, Climate Geochemistry Department, Mainz, Germany
[d] Institute of Earth Sciences, University of Lausanne, Switzerland
[e] Institute of Geological Sciences and Oeschger Center for Climate Change Research, University of Bern, Switzerland
[f] Department of Earth Science, ETH Zurich, Zurich, Switzerland
[g] NIOZ – Royal Netherlands Institute for Sea Research, Department of Ocean Systems, Texel, the Netherlands
[h] Faculty of Science, Department of Earth Sciences, Vrije Universiteit Amsterdam, Amsterdam, the Netherlands
[i] Lamont-Doherty Earth Observatory, Columbia University, Palisades, NY, USA

ARTICLE INFO

Article history:
Received 18 December 2020
Received in revised form
21 April 2021
Accepted 24 April 2021
Available online xxx

Handling Editor: I Hendry

Keywords:
Mineral dust
Dust grain size
Southern ocean
Southern westerly winds
Glacial
Interglacial dust variability

ABSTRACT

Downcore sediment grain-size records of mineral dust (2–10 μm) can provide key insights into changes in wind strength and source-area characteristics over glacial-interglacial timescales. However, so far, little is known about glacial-interglacial changes of dust grain size in the open Southern Ocean, which are potentially associated with changes in the strength and position of the southern westerly winds. Here, we analyzed the grain-size distributions of subantarctic deep-sea sediments from the Pacific (PS75/056–1) and Atlantic (ODP Site 1090) sectors of the Southern Ocean, downwind of the major Southern Hemisphere dust source regions. Dust mean grain sizes show opposite trends in the two Southern Ocean sectors. Larger glacial grain sizes are observed in the Pacific sector, while finer glacial grain sizes are observed in the Atlantic sector. In the South Pacific, larger mean dust grain sizes parallel higher Fe fluxes during glacials. In contrast, in the South Atlantic record increased glacial Fe fluxes coincide with a decrease in glacial mean dust grain sizes consistent with some Antarctic ice core records. Our results suggest that the opposing grain-size trends are the result of different responses to glacial conditions in the sources and of changing wind and transport patterns. For the South Pacific, a possible explanation of our results could be an intensification of wind strength over Australia enabling emission of larger dust particles. This strengthening would imply a northward shift of the westerlies which facilitated the transport of dust from enhanced and/or more Australian and New Zealand sources. For the Atlantic, the decreased glacial dust grain size could be the consequence of increased glacial activity in the Patagonian Andes, generating and supplying more and finer-grained dust from the exposed continental shelf to the South Atlantic. These findings indicate that more extensive studies of wind-blown sediment properties in the Southern Ocean can provide important insights on the timing and latitudinal extent of climatic changes in the sources and variations of transport to the Southern Ocean by the westerly winds.

1. Introduction

Atmospheric dust plays a key role in the global climate system through direct and indirect impacts on climate. Dust in the atmosphere influences the atmospheric radiation budget through scattering and absorbing solar radiation (Arimoto, 2001), and by acting as cloud condensation and ice nuclei (Twohy et al., 2009). In

* Corresponding author.
E-mail address: michelle.van.der.does@awi.de (M. van der Does).
[1] These authors contributed equally to the paper.

https://doi.org/10.1016/j.quascirev.2021.106978

addition, dust deposition affects marine biological productivity, and thus the global carbon cycle, through iron fertilization of high nutrient low chlorophyll (HNLC) regions (Martin, 1990). Southern Hemisphere westerly wind intensity and position are thought to play a crucial role in modulating glacial/interglacial CO_2 changes through their impact on Antarctic Circumpolar Current upwelling intensity and the delivery of iron-rich dust that stimulates marine biological production during glacial periods. In fact, some palaeoceanographic reconstructions suggest that iron fertilization of the Subantarctic Zone of the Southern Ocean can explain up to 40 ppmv of the atmospheric CO_2 decrease observed during ice ages (Jaccard et al., 2013; Martínez-García et al., 2014).

The emission of fine-grained material in dust source areas strongly depends on regional climatic conditions influencing soil and terrain properties, such as vegetation cover, rainfall intensity and local winds (Marticorena, 2014). Moreover, several studies have shown the importance of the extent of glaciation in high-latitude source areas for the total supply of increased fine-grained material for aeolian suspension (Sugden et al., 2009), and with that iron speciation which influences the bioavailability of dust supplied to the Southern Ocean (Shoenfelt et al., 2018). Dust transport to the Southern Ocean is controlled by large-scale atmospheric wind patterns at different altitudes within the southern westerly wind belt (SWW) as the main carrier of dust (Li et al., 2008). The amount and size of the deposited dust particles thus not only depends on wind speed, but also on several environmental factors including the aridity and areal extent of source regions, the grain size of source soil, proximity to the dust source and atmospheric residence time, and relative contributions of dry and wet dust deposition (Kohfeld et al., 2013; Újvári et al., 2016; Van der Does et al., 2020). The grain-size signature of dust can be further altered during transport by several atmospheric size-selecting processes including dry depositional processes such as gravitational settling and turbulent diffusion, as well as wet deposition such as in-cloud and below-cloud scavenging, or rainout and washout, respectively (Újvári et al., 2016), due to which coarse particles are generally deposited closer to the source, while finer dust particles are enabled to travel greater distances (Van der Does et al., 2016).

Antarctic ice cores provide valuable archives of dust deposition over several glacial/interglacial (G/IG) cycles. Paleoclimate reconstructions from the EPICA (European Project for Ice Coring in Antarctica) ice core at Dome C (EDC) in East Antarctica that cover the last ~800,000 years (800 kyr) reveal a ~25-fold increase in glacial dust fluxes compared to interglacial periods, in line with large changes in Antarctic temperature and CO_2 records (Lambert et al., 2008; Lüthi et al., 2008). However, the large glacial-interglacial amplitudes in Antarctic dust potentially overestimate the glacial enhancement of dust emission due to substantial changes in the hydrological cycle, which causes less dust to be deposited along its trajectory by wet deposition, and thus a larger proportion eventually reaches Antarctica (Petit and Delmonte, 2009; Markle et al., 2018). The provenance of dust in Antarctic ice cores has been studied and traced back to several sources in South America (Delmonte et al., 2010; Gili et al., 2017; Paleari et al., 2019; Struve et al., 2020), and Australia (Revel-Rolland et al., 2006), and additional knowledge of dust distribution in the Southern Hemisphere is based on modeling studies (Li et al., 2008; Albani et al., 2014; Neff and Bertler, 2015).

In several East-Antarctic ice core records, such as the EDC, Komsomolskaia and EPICA Dronning Maud Land (EDML) ice cores, dust records show decreasing dust grain size in parallel with increased dust fluxes during glacial periods, while another East-Antarctic ice core Dome B shows the opposite trend, with increased dust grain size during glacials (Delmonte et al., 2004; Wegner et al., 2015; Delmonte et al 2017). These contradicting grain-size trends are suggested to be linked to different atmospheric residence times due to different transport pathways and altitudes, while geochemical analyses revealed a common glacial dust provenance for all three ice cores (Delmonte et al., 2004).

High-resolution down-core dust records from the Southern Ocean indicate two to five times higher dust deposition rates in glacial periods compared to interglacial periods, coupled with higher export productivity (Anderson et al., 2014; Lamy et al., 2014; Martínez-García et al., 2014; Thöle et al., 2019). These records are mostly based on Fe and terrestrial biomarker contents, corrected for sediment focusing/winnowing using Th isotopes, thus allowing a direct quantitative estimation of dust supply to the Southern Ocean. Additional information on dust transport and deposition, such as wind speed and transport pathways, can be obtained from grain-size data (e.g. Holz et al., 2007). However, so far, little is known about grain-size distributions of dust in the Southern Ocean. A previous study comprises two sediment cores in the Tasman Sea, which show an increased proportion of coarse to fine dust populations, coinciding with substantially higher dust fluxes during glacial periods, as a result of enhanced dry deposition (Hesse and McTainsh, 1999). The authors argue that the increase in glacial dust transport and offshore deposition resulted from expanded source areas caused by reduced vegetation rather than increased wind strength. However, De Deckker et al. (2019) found evidence of decreased Holocene wind strength compared to previous glacial and interglacial periods, although this hypothesis is based on only two samples.

Here, we present grain-size distributions from two subantarctic sediment cores, located in the Pacific and Atlantic sectors of the Southern Ocean. Both sediment cores are located downwind of the major Southern Hemisphere dust source regions (Australia, New Zealand and South America, respectively) and are therefore ideal to study temporal and spatial dust transport to the Southern Ocean. Our aim is to improve our understanding of processes and mechanisms involved in Southern Ocean dust deposition possibly associated with changes in the strength and position of the SWW.

2. Material and methods

2.1. Core material and core locations

This study is based on two marine sediment records from the subantarctic Pacific and Atlantic sectors of the Southern Ocean (Fig. 1). South Pacific core PS75/056−1 (55.16°S; 114.79°W, 10.21 m core length at 3581 m water depth) was recovered during R/V *Polarstern* expedition ANT-XXVI/2, PS75, using a gravity corer (Gersonde, 2011). The site is located at the eastern flank of the southernmost East Pacific Rise within the Eltanin-Tharp Fracture Zone, ~130 nmi from the modern seafloor spreading axis. The site lies in the pathway of the Antarctic Circumpolar Current (ACC), ~170 nmi north of the modern mean position of the Subantarctic Front (SAF) in a zonal transition zone of the ACC. West of the site, the ACC and the associated fronts are strongly steered by the topography of seafloor spreading systems (Udintsev and Eltanin-Tharp Fracture Zone systems). Sediments predominantly consist of calcareous ooze during interglacial periods, with $CaCO_3$ values ranging from ~60 to ~80 wt %. During glacial periods, the sediment contains more siliceous microfossils, with maximum biogenic opal contents ranging from ~20 to ~40 wt % (Lamy et al., 2014). Glacial carbonate contents vary between ~20 and ~40 wt %. The oxygen-isotope stratigraphic age model of core PS75/056−1 (Ullermann et al., 2016) was updated by Basak et al. (2018), using a detailed

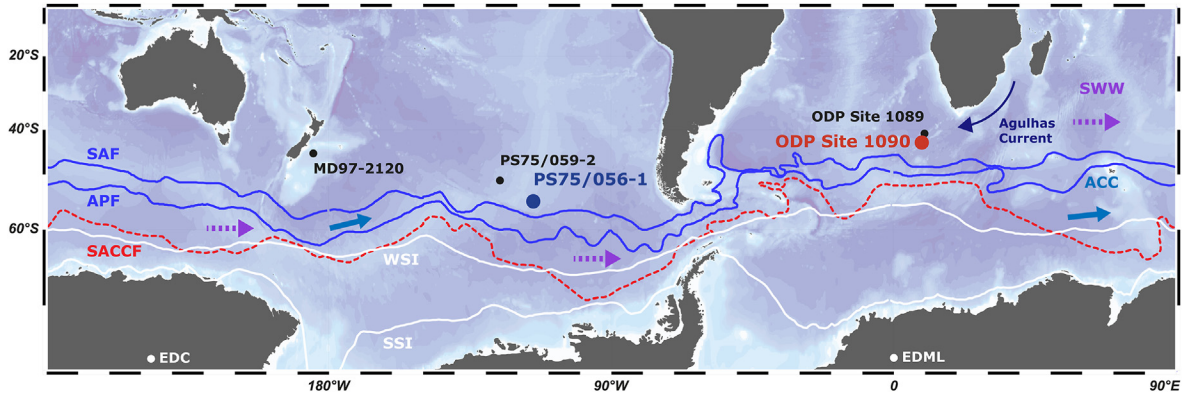

Fig. 1. Map of the Southern Ocean with core locations PS75/056–1 (blue) and ODP Site 1090 (red), and referenced ice- and sediment cores. Colored lines refer to mean positions of major front systems (Orsi et al., 1995). SAF: Subantarctic Front, APF: Antarctic Polar Front. SACCF: Southern Antarctic Circumpolar Current Front. Mean extension of winter and summer sea ice (WSI and SSI) are indicated by white lines (Comiso, 2003). Arrows indicate the flow direction of the Antarctic Circumpolar Current (ACC; blue), Agulhas Current (dark blue) and the direction of the Southern Westerly Winds (SWW; purple). The map was generated using Ocean Data View (Schlitzer, 2018). (For interpretation of the references to color in this figure legend, the reader is referred to the Web version of this article.)

correlation between the benthic $\delta^{18}O$ record and the $\delta^{18}O$ record of core MD 97–2120, located about 350 km off New Zealand. The sediments of core PS75/056–1 cover the last 260 kyr and reaches back to Marine Isotope Stage (MIS) 8.

ODP Site 1090 (42.91°S; 8.90°E, 3702 m water depth) was recovered during the Ocean Drilling Program Leg 177 expedition in the central part of the Subantarctic South Atlantic, at the southern flank of the Agulhas Ridge (Gersonde et al., 1999b). For the current study, we focus on the last glacial-interglacial cycle, i.e. the last 160 kyr, back to MIS6. The sediments of the uppermost 4.83 m composite depth at ODP Site 1090 predominantly consist of calcareous ooze, mud-bearing diatom and -nannofossil ooze. Biogenic opal and $CaCO_3$ contents were inferred from the nearby pre-site survey core PS2489-2 (Diekmann and Kuhn, 2002), which reveals biogenic opal contents up to 5 wt % in interglacials, whereas $CaCO_3$ reaches values up to 90 wt % during interglacials and up to 70 wt% in glacial periods. The age model of ODP Site1090 is described in Martínez-García et al. (2014). Briefly, the age model was generated by graphic correlation of the high resolution ^{230}Th-normalized Fe flux from ODP Site 1090 to the ice core dust reconstruction from EDC (Lambert et al., 2012), using the Antarctic Ice Core Chronology (Bazin et al., 2013; Veres et al., 2013).

2.2. Methods

2.2.1. Chemical leaching procedures of organic matter, biogenic opal and calcium carbonate

The chemical leaching to isolate the terrigenous fraction of sediment core PS75/056–1 was conducted at the Alfred Wegener Institute in Bremerhaven (AWI), whereas the ODP Site 1090 samples were processed at the Department of Earth Sciences at the Eidgenössische Technische Hochschule (ETH) in Zurich. Individual leaching procedures were applied to the sediment cores based on different sedimentary biogenic opal and $CaCO_3$ contents. For both methods the samples were carefully inspected under the microscope after each step of the procedure to ensure that biogenic particles were quantitatively removed.

Core PS75/056–1 was sampled at 5 cm intervals. Organic matter was removed by adding 20 mL H_2O_2 (35%) to ~5 g dry bulk sediment. The mixture was placed on a shaking table for at least 24 h or until the reaction between the sediment and the reagent ceased and excess H_2O_2 disintegrated into H_2O and O_2. Subsequently, the sediment was wet sieved to obtain the <63 μm fraction. Grain sizes >63 μm most likely represent large clay and mica minerals, whose platy shape allow for transport over greater distances (Stuut et al., 2005), although several studies have shown that so-called giant particles (>75 μm) can be entrained over 1000's of kilometers (Betzer et al., 1988; Van der Does et al., 2018). Given the high biogenic opal content of sediment core PS75/056–1 (up to 60 wt%), we developed a new leaching procedure to ensure complete removal of biogenic opal using NaOH, which is explained in detail in the Supplementary Information (SI). Briefly, it was found that 250 mL of 20% NaOH was most effective, which was added to ~1 g organic matter-free <63 μm fraction, heated, and rinsed. The biogenic opal-free samples were transferred into 125 mL transparent plastic beakers and filled up to 110 mL with demineralized (demi) water. Approximately 1 mL 10% HCl was added to remove calcium carbonate ($CaCO_3$), and the mixture was placed on a shaking table in a ventilation hood for 24 h, and the sediments subsequently settled for another 24 h. To avoid moving the plastic beakers and dispersing the settled particles, we used a water jet pump to remove the overlying supernatant. The rinsing process of the solution was repeated until the pH of the sediment was equal to the pH of the demi water.

Sediments from ODP Site 1090 were sampled at 1–2 cm intervals. $CaCO_3$ was removed by adding 5 mL HCl (10%) to approximately 100–300 mg sediment in 15 mL centrifuge tubes. The samples were centrifuged (5 min at 3000 rpm) and the supernatant was discarded. Subsequently, the samples were rinsed and centrifuged with 10 mL of demi water. Organic matter was removed by adding 5 mL H_2O_2 (34%), and the samples were transferred to a boiling water bath for 1 h. The samples were centrifuged and the supernatant was discarded, and subsequently rinsed. Biogenic opal (<5 wt %) was removed with 5 mL NaOH (10%). The samples were transferred to the boiling water bath for 30 min and rinsed to bring the pH to neutral.

2.2.2. Grain-size analysis

For core PS75/056–1, grain-size analysis was conducted on the <63 μm terrigenous fraction at the Royal Netherlands Institute for Sea Research (NIOZ). Prior to grain-size analysis, 20 mL 2% $Na_4P_2O_7 \bullet 10H_2O$ (sodium pyrophosphate) was added to each sample and placed on a shaking table for 24 h to completely disaggregate particles. The particle-size distributions were measured with a Beckman Coulter laser diffraction particle sizer LS13 320, which resulted in 116 size classes ranging from 0.04 to 2000 μm. To minimize the influence of gas bubbles, degassed water was used during analysis. The calculation of the particle sizes relies on the

Fraunhofer diffraction theory and the Polarization Intensity Differential Scattering (PIDS), for particles from 0.4 to 2000 μm and from 0.04 to 0.4 μm, respectively. In an earlier study, the reproducibility for this setup was described to be better than ±0.7 μm for the mean and ±0.6 μm for the median particle size (1σ) for the entire grain-size distribution of internal glass-bead standards, with the average standard deviation integrated over all the size classes better than ±4 vol% (Van der Does et al., 2016).

For ODP Site 1090, grain-size analysis was conducted on the terrigenous sediment fraction at ETH in Zürich. 48 h prior to the grain-size analysis, 10 mL 2% $Na_4P_2O_7 \bullet 10H_2O$ was added to each sample and occasionally resuspended, to completely disaggregate the sediment. The particle-size distributions were measured with a Malvern Mastersizer 2000 (laser diffraction), which resulted in 84 size classes ranging from 0.02 to 2000 μm.

The resulting grain-size distributions are expressed as volume percentage per size class (vol%). Grain size mean values for both cores for different size fractions were calculated following the Folk and Ward geometric graphical method (Folk and Ward, 1957) using the program *GRADISTAT* (Blott and Pye, 2001). Since the grain-size measurements for both cores were performed on different instruments, the grain-size bins of the output data differ slightly, and do not exactly match the boundaries of conventional size classifications. The defined boundaries of the used size fractions can be found in Table S1.

3. Results

Terrestrial biomarkers (long-chain n-alkanes) found in the sediments of PS75/056−1 and nearby core PS75/059−2, as well as for Pleistocene sediments at ODP Site 1090, reveal the presence of leaf-waxes, with a characteristic odd-over-even distribution typical for terrestrial plants, in the organic fraction of dust (Martínez-García et al., 2009; Lamy et al., 2014). This implies minimal input from ice rafted debris (IRD), which typically present an n-alkane distribution characterized by no clear odd-over-even predominance (Villanueva et al., 1997). In addition, the strong similarity between these terrestrial n-alkanes and the bulk sedimentary Fe content suggest that the fine lithogenic fraction is transported to the core sites via winds, likely from mid-latitude source areas (Martínez-García et al., 2009; Lamy et al., 2014). Therefore, contributions from IRD affecting the grain-size distributions can be considered negligible. However, our new high-resolution grain size data presented below suggest that IRD may have represented an important secondary source of terrigenous material to ODP Site 1090 during MIS 3. Current-driven transport of sediments may also have played a role at our core sites, but the largest part of the grain-size distributions, the fine silt fraction (2−10 μm), is cohesive and forms aggregates and is therefore not affected by current redistribution at the seafloor (McCave et al., 1995).

For core PS75/056−1, all samples show a bimodal grain-size distribution with a primary mode at ~4 μm and a secondary mode at ~30 μm (Fig. 2A). Long-range transported dust is mostly limited to <30 μm (Ryder et al., 2013; Van der Does et al., 2016), although in some cases coarser dust particles seem to persist (Ryder et al., 2019). For core PS75/056−1, this could be the case for the particles observed in the secondary mode, for which different transport processes could possibly play a role (Van der Does et al., 2018). Unfortunately, there is currently no grain-size data of modern dust deposition in the Southern Ocean available. An alternative explanation is that this secondary peak is caused by a smaller influence of current sorting (McCave et al., 1995). It is unlikely that this secondary mode represents an input of coarse IRD particles since they are present in all samples, and we would expect the input of IRD to fluctuate over the glacial/interglacial period. On average, about 90 vol % of the total sediment is concentrated in the clay (0−2 μm, 38%) and fine silt (2−10 μm, 52%) fractions, while the medium to coarse silt (10−63 μm) fraction contributes on average only 10 vol % (Fig. 2B). Since the samples were sieved to obtain the <63 μm fraction, on average less than 0.1% was measured as >63 μm, and this fraction is therefore considered negligible. Four (out of 183) samples (lighter-colored samples in Fig. 2A) that did not fit the patterns of the remaining samples are considered measurement outliers. These are single samples with very different grain size, that are not statistically relevant in the large total number of samples – they are displayed in the Supplementary Information (Fig. S2), but excluded from further interpretations in the following sections.

The sediment record at ODP Site 1090 contains mostly unimodal grain-size distributions with a primary mode at ~3 μm that is similar to sediment core PS75/056−1, whereas some samples, mostly from MIS 3 (26 out of 308 samples), reveal a primary mode at ~9 μm (lighter-colored samples in Fig. 2A). The clay (0−2 μm, 29%) and fine silt (2−10 μm, 50%) fractions contribute on average 79 vol % to the distributions, while on average 21 vol % is concentrated in the medium to coarse silt (10−63 mm) fraction (Fig. 2C). The >63 μm fraction comprises on average less than 1%. Overall, the grain-size distributions show only very minor variations throughout the record, with the exception of MIS3.

Increased grain sizes during MIS 3 at ODP Site 1090 may indicate a different or secondary source of terrestrial material, such as increased input of IRD. This additional contribution may explain the elevated dust flux estimates obtained for ODP Site 1090 and other South Atlantic records during MIS 3 compared to Antarctic ice cores (Fig. 3C and D) (Anderson et al., 2014). Kanfoush et al. (2002) also found millennial-scale IRD events of great magnitude and frequency during MIS 3 at ODP Site 1094, and Starr et al. (2021) argue that increased fluxes of IRD lead relative to global climate, and can reach the position of our core location in the South Atlantic. The causes of the appearance of this additional terrigenous source during MIS 3, and not during the colder MIS 2, 4 and 6 remains enigmatic at this point. Future studies using terrigenous source tracers (such as Sr, Nd or Pb isotopes, and/or organic biomarkers) may help to shed light on the origin of this additional terrigenous source. Due to the highly unsorted grain size distribution of IRD, it would be very difficult to eliminate the effect on the (dust particle) size distributions. In any case, it is clear that the grain-size distributions during MIS 3 are not suited for describing dust particle size since the origin of these terrigenous particles remains unclear. Therefore, they are not considered further into the discussion, but are displayed in the Supplementary Information (Fig. S2) and reported in the data files.

Since the sediments studied here are recovered from the ocean floor, besides properties of the continental source soil of the dust and multiple size-selecting processes during dust emission and long-range transport (Újvári et al., 2016), the particle size of the studied terrigenous fraction may be influenced by sorting after deposition on the seafloor due to bottom currents. This is particularly important in the Southern Ocean as the ACC reaches the seafloor over vast areas (McCave et al., 2014). Medium to coarse silt (or sortable silt; 10−63 μm) is sensitive to sediment sorting by bottom currents owing to its non-cohesive behavior, and is often used as a paleocurrent indicator (McCave et al., 1995; Wu et al., 2019). Clay mineral distribution from the clay fraction (<2 μm) is also often used to display current transport (Petschick et al., 1996). The fine silt fraction (2−10 μm) is not affected by current redistribution at the seafloor, as this sediment fraction is cohesive and forms aggregates (McCave et al., 1995). Particles larger than 20 μm are likely not related to aeolian dust, but rather to current-driven

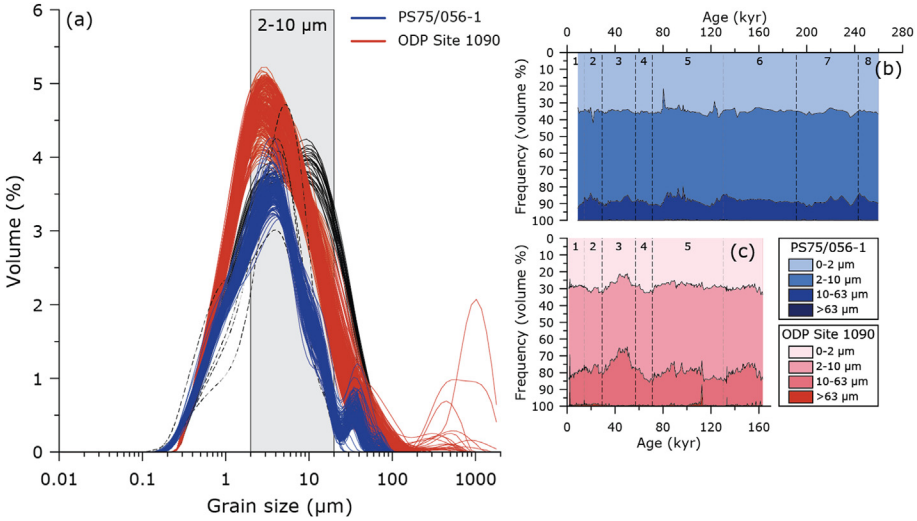

Fig. 2. A: Grain-size distributions of terrigenous sediments of PS75/056−1 (blue) and ODP Site 1090 (red). Each line represents a single sample. For PS75/056−1, grain sizes were measured on the <63 µm fraction. The black lines represent outliers (PS75/056−1, dashed lines) and MIS3 samples (ODP Site 1090, solid lines). The grey bar marks the assumed dust (2−10 µm) fraction. B & C: Composition of standard size fractions for sediments of PS75/056−1 (B) and ODP Site 1090 (C), versus age. Dashed lines and numbers at the top indicate the Marine Isotope Stages. (For interpretation of the references to color in this figure legend, the reader is referred to the Web version of this article.)

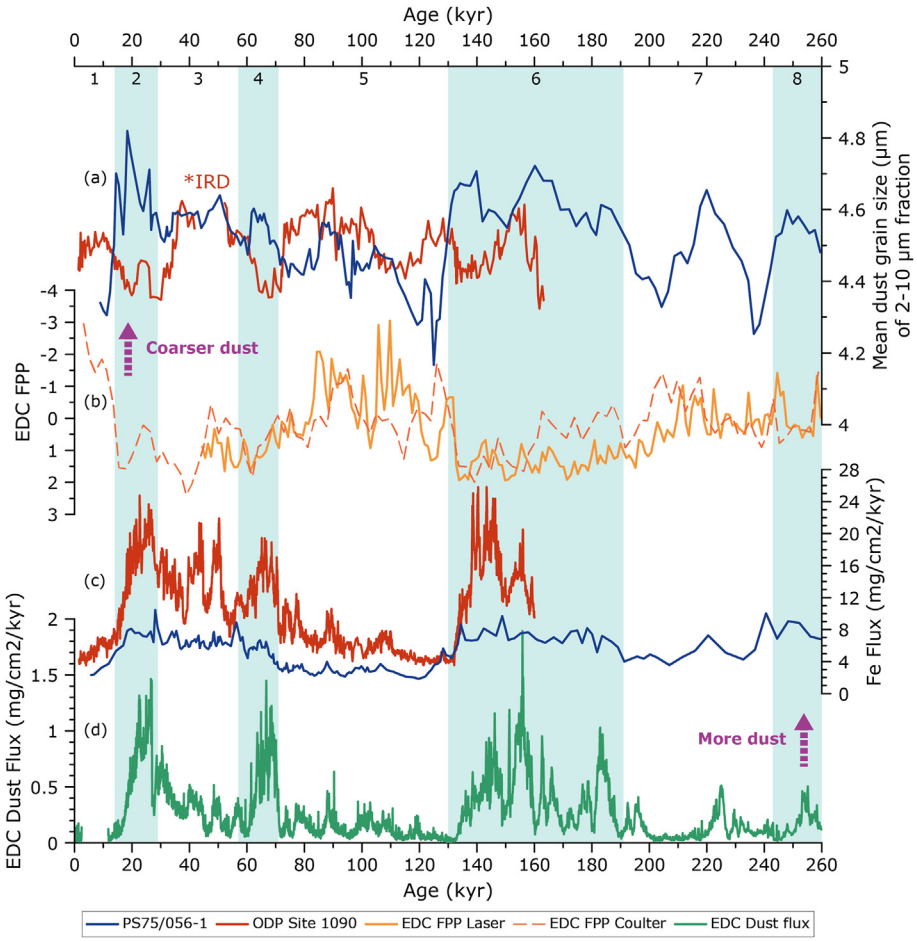

Fig. 3. A: Mean grain size (2−10 µm fraction) of sediments of PS75/056−1 in the Pacific sector of the Southern Ocean (blue) and ODP Site 1090 in the Atlantic sector (red). Grain sizes for ODP Site 1090 during MIS 3 are omitted as they likely represent an alternative sediment source, as well as four coarse outliers of PS75/056−1 (displayed in Fig. S2). B: Fine Particle Percentage (FPP; percentage of particles between 1 and 2 µm) of EDC ice core inferred by both laser particle sizer (solid line) and Coulter Counter (dashed line), where smaller values correspond to coarser-grained dust (both from Lambert et al., 2008). C: Fe flux in sediments of core PS75/056−1 (blue; Lamy et al., 2014) and ODP Site 1090 (red; Martínez-García et al., 2014), representing dust deposition. D: EDC dust flux (Lambert et al., 2012). Both EDC records are plotted on the most recent AICC2012 chronology (Veres et al., 2013). Marine Isotope Stages are indicated at the top, with blue bars highlighting glacial conditions. (For interpretation of the references to color in this figure legend, the reader is referred to the Web version of this article.)

transport or contributions of IRD. An evaluation of different size fraction reveals that they all roughly show the same glacial/interglacial trends, and therefore, we suspect that the contributions of current-redistributed sediments and IRD play only a minor role. However, based on the arguments given above, we consider the trends of the dust fraction to be best represented by the mean grain size of the 2–10 μm fraction.

For core PS75/056–1 in the Pacific sector of the Southern Ocean, mean dust grain sizes vary between 4.17 μm and 4.81 μm, and four outliers of 4.53–5.03 μm. Although the difference between the highest and lowest mean dust grain size amounts to only 0.62 μm, a distinct G/IG pattern is present, with generally coarser dust during glacial stages compared to interglacial stages (Fig. 3A).

At ODP Site 1090 in the Atlantic sector of the Southern Ocean, mean dust grain sizes range between 4.32 μm and 4.66 μm, very similar to sediment core PS75/056–1 in the South Pacific. The range between the highest and lowest mean dust grain size (0.34 μm), without considering the coarser-grained MIS3 samples, is slightly smaller but similar to sediment core PS75/056–1 (0.65 μm). Grain sizes are generally coarser in the South Atlantic sediments compared to the South Pacific sediments over G/IG timescales (Fig. 3A). Interestingly, we also observe an opposite G/IG grain size pattern in the South Atlantic compared to the South Pacific, i.e. interglacial periods in the Atlantic show coarser dust compared to glacial periods. The opposing grain-size trends between the two sectors are particularly evident during the cold glacial stages MIS 2, MIS 4 and MIS 6. In the next sections, we explore the mechanism(s) that may be responsible for the opposing G/IG dust grain-size patterns in the Pacific and Atlantic sectors of the Southern Ocean.

4. Discussion

Previous studies have shown that both cores were characterized by increased terrigenous fluxes and Fe accumulation during glacial periods (Martínez-García et al., 2011, 2014; Lamy et al., 2014; Shoenfelt et al., 2018), consistent with enhanced glacial dust deposition in both the South Atlantic and the South Pacific when compared to interglacial periods (Fig. 3C). These studies have suggested that bulk sediment Fe records from the Atlantic and Pacific sectors of the Southern Ocean also correlate with Antarctic dust accumulation, CO_2 and temperature records over G/IG timescales (Lambert et al., 2008, 2012; Lüthi et al., 2008).

4.1. Glacial/interglacial dust variability to the pacific sector of the Southern Ocean (PS75/056–1)

The geographical location in the Subantarctic Zone east of the East Pacific rise, and the prevailing direction of the SWW, suggest that Australia and/or New Zealand represent the major potential source areas. This interpretation is consistent with provenance studies using surface sediments of the South Pacific, which suggest that, despite broad geochemical similarities between Australian, New Zealand and southern South American dust sources, the Lake Eyre Basin in southeast Australia was a major dust supplier to the Pacific sector of the Southern Ocean during the Holocene (Wengler et al., 2019). Model-based studies of modern dust distribution in the Southern Hemisphere showed that approximately 86% of the dust in the South Pacific originates from Australian dust sources (Li et al., 2008).

Contrastingly, during the LGM, New Zealand represented an important secondary source of dust to the Southern Ocean and Antarctica (Lamy et al., 2014; Neff and Bertler, 2015; Durand et al., 2017), and due to the geographic location of core PS75/056–1, downwind of New Zealand, it could have contributed to increased South Pacific glacial dust accumulation and coarser grain sizes observed in core PS75/056–1, also due to the more proximal location to the core site compared to Australian sources. Increased erosion and/or weathering during glacial periods was inferred from marine sediments on the eastern side of New Zealand's South Island, and is interpreted as a result of the glacial ice coverage (Cogez et al., 2015; Durand et al., 2017), leading to enhanced dust availability.

In addition to an increased contribution of New Zealand dust to the South Pacific during glacial periods, another potential mechanism accounting for enhanced glacial Fe accumulation combined with increased mean dust grain sizes in Pacific core PS75/056–1 (Fig. 3A, C) relates to increased dust availability in Australian source areas, in combination with source area characteristics or transport mechanisms that favored the emission and subsequent transport of larger dust particles. In such a scenario, enhanced atmospheric dustiness may be related to climatic conditions in the source (e.g. increased wind strength, reduced precipitation and sparser vegetation cover), leading to expanded arid areas that favored enhanced dust production over central and southeast Australia (Hesse and McTainsh, 1999). A possible wind strengthening would imply a northward shift of the SWW. Subsequently, decreased rain-out of (coarse) dust particles along the SWW trajectory results in longer atmospheric residence times (Markle et al., 2018). Alternatively, increased glacial dust grain size could be the result of enhanced wind strength, transporting larger dust particles, which agrees with the majority of observations supporting increased strength and/or more northern position of the SWW (Kohfeld et al., 2013; Lamy et al., 2015, 2019), although other explanations of the observed data cannot be ruled out (Kohfeld et al., 2013). Struve et al. (2020) found Central South America to be an important source of dust to the South Pacific Subantarctic Zone during the LGM via circum-Antarctic dust transport. However, during this long-range transport it is unlikely that coarse particles would have persisted, and therefore an important contribution of South American sources to our core site in the South Pacific does not match our observation of coarser dust deposition during glacial stages. In summary, coarser glacial dust particles in combination with increased deposition fluxes observed in the South Pacific could be the result of a New Zealand contribution proving more and coarser dust as a more proximal source, increased dust availability from Australian sources in combination with enhanced wind strength of the SWW, and/or decreased rain out of coarse particles along their trajectory towards the core location. A detailed provenance study should give more information on the most dominant of these processes.

4.2. Glacial/interglacial dust variability to the atlantic sector of the Southern Ocean (ODP site 1090)

Similar to the sediment record from the Pacific sector of the Southern Ocean, increased Fe and terrestrial biomarker accumulation during glacial periods indicates enhanced dust deposition at ODP Site 1090 in the South Atlantic (Fig. 3C). Martínez-García et al. (2009) suggested that dust supply is the most likely transport mechanism of terrigenous material to ODP Site 1090. The geographical position of ODP Site 1090 and the prevailing direction of the SWW make southern South America the most prominent potential source area. This corresponds with model-based investigations of modern and LGM dust distribution in the Southern Hemisphere, revealing that ODP Site 1090 lies directly below the southern South American dust plume (Li et al., 2008, 2010; Albani et al., 2012). In particular, 90% of the total modern dust deposited in the South Atlantic originates from South American sources (Li et al., 2008). In general, Fe fluxes to our South Atlantic record are ~3 times higher during glacial periods and ~2 times higher during interglacial periods, compared to the South Pacific record, but the general

trends of increased dust deposition during glacials are similar (Fig. 3C).

Several studies suggest that current-driven transport could have been an important contribution to the terrigenous sediments to the South Atlantic. Noble et al. (2012) inferred that Holocene terrigenous fluxes can be explained by a predominant sediment supply from South Africa via the Agulhas current, based on a suite of sediment records from ODP Leg 177 (including ODP Site 1090). The same authors found similar or increased terrigenous fluxes for the LGM, which they interpreted as evidence of sediment transport driven by the ACC (Noble et al., 2012). In addition, Kuhn and Diekmann (2002) concluded based on sediments of nearby ODP Site 1089 (Fig. 1) that the terrigenous fraction was mainly supplied from African sources by current-driven transport. However, these sediments were collected from a drift deposit in the deep Cape Basin (Gersonde et al., 1999a), and the sediments from ODP Site 1090 were retrieved from the southern flank of the Agulhas Ridge which is less influenced by current-driven transport (Martínez-García et al., 2011). Also, several lines of evidence suggest that the observed grain size change reflects that of atmospheric dust particles. First, the G/IG grain size pattern observed at ODP Site 1090 mirrors that reported in Antarctic ice cores from EDC. Second, the pattern of dust fluxes at ODP Site 1090 is remarkably similar to those from Antarctic ice cores over the past 800,000 years (Martínez-García et al., 2011). Lastly, ^{230}Th isotope measurements show little evidence of sediment focusing or winnowing at the location of ODP Site 1090 (Martínez-García et al., 2009).

Having a similar dust source, the east Antarctic EDC ice core dust record depicts similar G/IG dust variability as the sediment record at ODP Site 1090, with increased dust fluxes and decreased grain sizes during glacial periods (Fig. 3B, D) (Lambert et al., 2008). This trend was also observed in the EPICA Dronning Maud Land (EDML) ice core, with more and slightly smaller dust particles during the glacial (Wegner et al., 2015). Grain-size distributions of Antarctic ice-core dust typically have modal grain sizes of 2 μm, with a maximum particle diameter of about 5 μm and very little variability (Delmonte et al., 2020). In Fig. 3B, the EDC grain sizes are presented as Fine Particle Percentage (FPP), which is defined as the particles with diameters between 1 and 2 μm, and is inversely correlated with the modal values of their grain-size distributions (Lambert et al., 2008). Another East-Antarctic ice core (Dome B) shows opposite glacial dust grain sizes, and these differences were found to be caused by different altitudes at which the dust is transported towards Antarctica (Delmonte et al., 2004), with dust transported to EDC having trajectories at higher altitudes than dust transported to Dome B. This could also have played a role for the sediments found at ODP Site 1090.

Geochemical analysis of South American potential source areas reveal that during glacial periods, Patagonian dust sources were the main dust supplier to east Antarctica (Delmonte et al., 2017). This is in agreement with dust modeling studies that show that Patagonian sources dominated dust deposition over Antarctica during the LGM (Albani et al., 2012). Peaks of dust concentration in Antarctic ice cores correspond to increased meltwater discharge from Patagonian glaciers onto outwash plains, where dust can easily be mobilized (Sugden et al., 2009). During the LGM, glacial outwash plains are thought to be extended across the continental shelf due to lower sea level, supplying vast amounts of sediments and acting as a major source of dust (Basile et al., 1997; Sugden et al., 2009; Noble et al., 2012; Delmonte et al., 2017; Paleari et al., 2019). At the same time, a diminished hydrological cycle during glacial periods over the Atlantic sector of the Southern Ocean reduced wet deposition processes and increased the particle lifetime during atmospheric transport, leading to a ~25-fold increase in EDC Antarctic glacial dust fluxes (Fig. 3D) (Lambert et al., 2012; Markle et al., 2018). These same mechanisms could also explain the increased glacial dust fluxes at ODP Site 1090, which receives dust from the same South American sources. Increased South American glaciation could also have contributed to the overall finer particle sizes of the source sediments and the generation of glacial flour (Sugden et al., 2009), leading to the distinct finer dust particle sizes observed in glacial periods at ODP Site 1090 as well as an increase in dust deposition. This effect was likely smaller for the South Pacific dust sources as glaciation in Australia was limited (Barrows et al., 2001), and although New Zealand's sources experienced stronger glaciation (Hesse and McTainsh, 2003), they were likely too small to make a large contribution to the sediment record at PS75/056−1 (Wu et al., 2021).

An alternative explanation of the grain size data relates to the shift of potential source areas within South America. As South American dust sources extend along a ~4000 km latitudinal band from the Puna-Altiplano Plateau in the north to Patagonia in the south (Gili et al., 2017), latitudinal variations of the SWW could have resulted in changing source areas. During glacial periods, the SWW likely shifted northward, which could have resulted in a diminished contribution from Patagonian dust sources (Lamy et al., 2019). Therefore, the (relative) contribution from more northern dust sources may have increased, increasing the travel distance and atmospheric residence time to ODP Site 1090, and ultimately delivering finer glacial dust particles as a result of coarse-particle fallout along its longer trajectory before reaching the core location.

During interglacial periods, the southern Altiplano area in the northern part of southern South America is hypothesized to be the main source of dust to east Antarctic ice cores (Gili et al., 2017). Ice-core data from the central Andes reveal drier conditions in the Altiplano area during the Holocene opposed to wetter conditions during the last glacial (Fornace et al., 2014). However, this change in dust source would then also be visible in all Antarctic ice cores, but instead these show opposite dust grain-size trends which are attributed to different transport pathways and altitudes (Delmonte et al., 2004). It is therefore less likely that changed dust provenances would explain the G/IG grain-size trend at ODP Site 1090, but rather different atmospheric trajectories and altitudes of dust transport in combination with a greater dust supply due to the greater glacial extend of sources, the expanded outwash plains across the continental shelf and increased availability of finer-grained material in those sources, as seen in Antarctic ice core records (Delmonte et al., 2004, 2017).

5. Conclusions

We investigated down-core grain-size variations of two marine sediment records from the subantarctic Pacific and Atlantic sectors of the Southern Ocean. For this we focused on the mean of the 2−10 μm fraction, which is the fraction least affected by current redistribution, to best represent variability in dust grain size.

Our data reveal opposing down-core grain size records in the Pacific and Atlantic sectors of the Southern Ocean. The grain-size record of PS75/056−1 in the South Pacific is characterized by larger mean dust grain sizes during glacial periods, in parallel with increased glacial Fe accumulation. This could be the result of drier glacial climate conditions, favoring enhanced dust mobilization in the Australian sources, but also decrease the rain-out of coarse particles along its trajectory towards the core location. An intensification of wind strength over Australia could have enabled the emission of larger dust particles. In addition, with New Zealand as a more prominent source during glacials, dust derived from those source areas would have a shorter atmospheric transport time to the core location and thus coarser-grained dust particles could have been transported to the core site PS75/056−1. Taken together, our

inferences would be consistent with previous studies showing a northward shift or extension of the SWW over the Australian/New Zealand sector. Provenance studies should give more information on the most dominant of these processes.

The grain-size data from the South Atlantic (and published records of Antarctic ice cores from EDC) show an opposite pattern to the South Pacific, with decreased mean dust grain sizes during glacial periods, whereas increased glacial Fe fluxes indicate enhanced dust availability in southern South American sources. During glacial periods, dust was predominantly derived from Patagonia, where increased outwash plains over the continental shelf supplied more sediments, but expanded glacial SWW coupled with a diminished core over Patagonia likely hampered the erosion of coarse dust particles. In addition, due to enhanced glacial conditions, the material produced could have been finer-grained than during interglacial periods. Similar to was is observed in East-Antarctic ice cores even further downwind, the finer dust particles during glacial periods could have been enhanced due to atmospheric transport at higher altitudes in the atmosphere.

Overall, our study suggests that grain-size changes observed in the Pacific and Atlantic sectors of the Southern Ocean are the result of different responses of dust emission under glacial climate conditions and changes in transport pathways. Dust deposited in the Pacific sector of the Southern Ocean is plausibly associated with increased aridity and wind strength at the source, leading to the transport of coarser-grained dust particles. In South America, enhanced glacial erosion led to the mobilization of finer-grained material, which was then transported to the Atlantic sector of the Southern Ocean. Although down-core dust provenance studies are required to confirm the origin of dust particles, our data suggest that east-west and north-south down-core grain-size records in the Pacific and Atlantic sectors of the Southern Ocean could provide important insights on the timing and extent of glaciation in the dust source areas and changes in the westerly winds.

Author statement

Michèlle van der Does: Formal analysis, Writing – original draft, Visualization, Marc Wengler: Methodology, Investigation, Writing – original draft, Frank Lamy: Conceptualization, Writing – review & editing, Supervision, Funding acquisition, Alfredo Martínez-García: Conceptualization, Methodology, Resources, Writing – review & editing, Samuel L. Jaccard: Methodology, Resources, Writing – review & editing, Gerhard Kuhn: Conceptualization, Writing – review & editing, Verena Lanny: Investigation, Writing – review & editing, Jan-Berend W. Stuut: Resources, Writing – review & editing, Gisela Winckler: Conceptualization, Writing – review & editing

Data availability

Data used in this manuscript is available at https://doi.pangaea.de/10.1594/PANGAEA.929115.

Declaration of competing interest

The authors declare that they have no known competing financial interests or personal relationships that could have appeared to influence the work reported in this paper.

Acknowledgements

The captains, crew and scientists of R/V *Polarstern* (ANT-XXVI/2, PS75) and *JOIDES Resolution* (ODP Leg 177) are thanked for sample collection and logistical efforts. We are grateful to R. Fröhlking-Teichert and S. Wiebe for technical assistance. This study is part of the project "Polar Regions and Coasts in the changing Earth System (PACES II)" of the Alfred Wegener Institute (AWI) Helmholtz Center for Polar and Marine Research, and the AWI Strategy Fund Project "DustIron". We acknowledge financial support for this work through AWI and MARUM, Center for Marine Environmental Sciences. SLJ acknowledges support from the Swiss National Science Foundation (SNSF - grant PP00P2-144811).

Appendix A. Supplementary data

Supplementary data to this article can be found online at https://doi.org/10.1016/j.quascirev.2021.106978.

References

Albani, S., Mahowald, N.M., Delmonte, B., Maggi, V., Winckler, G., 2012. Comparing modeled and observed changes in mineral dust transport and deposition to Antarctica between the Last Glacial Maximum and current climates. Clim. Dynam. 38 (9), 1731–1755. https://doi.org/10.1007/s00382-011-1139-5.

Albani, S., Mahowald, N.M., Perry, A.T., Scanza, R.A., Zender, C.S., Heavens, N.G., Maggi, V., Kok, J.F., Otto-Bliesner, B.L., 2014. Improved dust representation in the community atmosphere model. J. Adv. Model. Earth Syst. 6 (3), 541–570. https://doi.org/10.1002/2013MS000279.

Anderson, R.F., Barker, S., Fleisher, M., Gersonde, R., Goldstein, S.L., Kuhn, G., Mortyn, P.G., Pahnke, K., Sachs, J.P., 2014. Biological response to millennial variability of dust and nutrient supply in the Subantarctic South Atlantic Ocean. Phil. Trans. Math. Phys. Eng. Sci. 372 (2019), 20130054. https://doi.org/10.1098/rsta.2013.0054.

Arimoto, R., 2001. Eolian dust and climate: relationships to sources, tropospheric chemistry, transport and deposition. Earth Sci. Rev. 54 (1), 29–42. https://doi.org/10.1016/S0012-8252(01)00040-X.

Barrows, T.T., Stone, J.O., Fifield, L.K., Cresswell, R.G., 2001. Late Pleistocene glaciation of the kosciuszko massif, snowy mountains, Australia. Quat. Res. 55 (2), 179–189. https://doi.org/10.1006/qres.2001.2216.

Basak, C., Fröllje, H., Lamy, F., Gersonde, R., Benz, V., Anderson, R.F., Molina-Kescher, M., Pahnke, K., 2018. Breakup of last glacial deep stratification in the South Pacific. Science 359 (6378), 900–904. https://doi.org/10.1126/science.aao2473.

Basile, I., Grousset, F.E., Revel, M., Petit, J.R., Biscaye, P.E., Barkov, N.I., 1997. Patagonian origin of glacial dust deposited in East Antarctica (Vostok and Dome C) during glacial stages 2, 4 and 6. Earth Planet Sci. Lett. 146 (3), 573–589. https://doi.org/10.1016/S0012-821X(96)00255-5.

Bazin, L., Landais, A., Lemieux-Dudon, B., Toyé Mahamadou Kele, H., Veres, D., Parrenin, F., Martinerie, P., Ritz, C., Capron, E., Lipenkov, V., Loutre, M.F., Raynaud, D., Vinther, B., Svensson, A., Rasmussen, S.O., Severi, M., Blunier, T., Leuenberger, M., Fischer, H., Masson-Delmotte, V., Chappellaz, J., Wolff, E., 2013. An optimized multi-proxy, multi-site Antarctic ice and gas orbital chronology (AICC2012): 120–800 ka. Clim. Past 9 (4), 1715–1731. 10.5194/cp-9-1715-2013.

Betzer, P.R., Carder, K.L., Duce, R.A., Merrill, J.T., Tindale, N.W., Uematsu, M., Costello, D.K., Young, R.W., Feely, R.A., Breland, J.A., Bernstein, R.E., Greco, A.M., 1988. Long-range transport of giant mineral aerosol-particles. Nature 336 (6199), 568–571. https://doi.org/10.1038/336568a0.

Blott, S.J., Pye, K., 2001. GRADISTAT: a grain-size distribution and statistics package for the analysis of unconsolidated sediments. Earth Surf. Process. Landforms 26 (11), 1237–1248. https://doi.org/10.1002/esp.261.

Cogez, A., Meynadier, L., Allègre, C., Limmois, D., Herman, F., Gaillardet, J., 2015. Constraints on the role of tectonic and climate on erosion revealed by two time series analysis of marine cores around New Zealand. Earth Planet Sci. Lett. 410, 174–185. https://doi.org/10.1016/j.epsl.2014.11.029.

Comiso, J.C., 2003. Warming trends in the arctic from clear sky satellite observations. J. Clim. 16 (21), 3498–3510. 10.1175/1520-0442(2003)016<3498:Wtitaf>2.0.Co;2.

De Deckker, P., Barrows, T.T., Stuut, J.B.W., van der Kaars, S., Ayress, M.A., Rogers, J., Chaproniere, G., 2019. Land–sea correlations in the Australian region: 460 ka of changes recorded in a deep-sea core offshore Tasmania. Part 2: the marine compared with the terrestrial record. Aust. J. Earth Sci. 66 (1), 17–36. https://doi.org/10.1080/08120099.2018.1495101.

Delmonte, B., Andersson, P.S., Schöberg, H., Hansson, M., Petit, J.R., Delmas, R., Gaiero, D.M., Maggi, V., Frezzotti, M., 2010. Geographic provenance of aeolian dust in East Antarctica during Pleistocene glaciations: preliminary results from Talos Dome and comparison with East Antarctic and new Andean ice core data. Quat. Sci. Rev. 29 (1), 256–264. https://doi.org/10.1016/j.quascirev.2009.05.010.

Delmonte, B., Paleari, C.I., Andò, S., Garzanti, E., Andersson, P.S., Petit, J.R., Crosta, X., Narcisi, B., Baroni, C., Salvatore, M.C., Baccolo, G., Maggi, V., 2017. Causes of dust size variability in central east Antarctica (Dome B): atmospheric transport from expanded south American sources during marine isotope stage 2. Quat. Sci. Rev. 168, 55–68. https://doi.org/10.1016/j.quascirev.2017.05.009.

Delmonte, B., Petit, J.R., Andersen, K.K., Basile-Doelseh, I., Maggi, V., Lipenkov, V.Y., 2004. Dust size evidence for opposite regional atmospheric circulation changes

over east Antarctica during the last climatic transition. Clim. Dynam. 23 (3–4), 427–438. https://doi.org/10.1007/s00382-004-0450-9.
Delmonte, B., Winton, H., Baroni, M., Baccolo, G., Hansson, M., Andersson, P., Baroni, C., Salvatore, M.C., Lanci, L., Maggi, V., 2020. Holocene dust in East Antarctica: provenance and variability in time and space. Holocene 30 (4), 546–558. https://doi.org/10.1177/0959683619875188.
Diekmann, B., Kuhn, G., 2002. Sedimentary record of the mid-Pleistocene climate transition in the southeastern South Atlantic (ODP Site 1090). Palaeogeogr. Palaeoclimatol. Palaeoecol. 182 (3), 241–258. https://doi.org/10.1016/S0031-0182(01)00498-9.
Durand, A., Chase, Z., Noble, T.L., Bostock, H., Jaccard, S.L., Kitchener, P., Townsend, A.T., Jansen, N., Kinsley, L., Jacobsen, G., Johnson, S., Neil, H., 2017. Export production in the new-zealand region since the last glacial maximum. Earth Planet Sci. Lett. 469, 110–122. https://doi.org/10.1016/j.epsl.2017.03.035.
Folk, R.L., Ward, W.C., 1957. Brazos river bar: a study in the significance of grain size parameters. J. Sediment. Res. 27 (1), 3–26. https://doi.org/10.1306/74D70646-2B21-11D7-8648000102C1865D.
Fornace, K.L., Hughen, K.A., Shanahan, T.M., Fritz, S.C., Baker, P.A., Sylva, S.P., 2014. A 60,000-year record of hydrologic variability in the Central Andes from the hydrogen isotopic composition of leaf waxes in Lake Titicaca sediments. Earth Planet Sci. Lett. 408, 263–271. https://doi.org/10.1016/j.epsl.2014.10.024.
Gersonde, R., 2011. The expedition of the Research vessel "polarstern" to the polar South Pacific in 2009/2010 (ANT-XXXVI/2 - BIPOMAC). Berichte zur Polar und Meeresforschung 632. https://doi.org/10.2312/BzPM_0632_2011.
Gersonde, R., Hodell, D.A., Blum, P., 1999a. Site 1089, chapter 4. In: Proceedings of the Ocean Drilling Program, vol. 117. https://doi.org/10.2973/odp.proc.ir.177.104.1999.
Gersonde, R., Hodell, D.A., Blum, P., 1999b. Site 1090, chapter 5. In: Proceedings of the Ocean Drilling Program, vol. 117. https://doi.org/10.2973/odp.proc.ir.177.105.1999.
Gili, S., Gaiero, D.M., Goldstein, S.L., Chemale, F., Jweda, J., Kaplan, M.R., Becchio, R.A., Koester, E., 2017. Glacial/interglacial changes of Southern Hemisphere wind circulation from the geochemistry of South American dust. Earth Planet Sci. Lett. 469, 98–109. https://doi.org/10.1016/j.epsl.2017.04.007.
Hesse, P.P., McTainsh, G.H., 1999. Last glacial maximum to early Holocene wind strength in the mid-latitudes of the southern Hemisphere from aeolian dust in the Tasman Sea. Quat. Res. 52 (3), 343–349. https://doi.org/10.1006/qres.1999.2084.
Hesse, P.P., McTainsh, G.H., 2003. Australian dust deposits: modern processes and the Quaternary record. Quat. Sci. Rev. 22 (18), 2007–2035. https://doi.org/10.1016/S0277-3791(03)00164-1.
Holz, C., Stuut, J.B.W., Henrlch, R., Meggers, H., 2007. Variability in terrigenous sedimentation processes off northwest Africa and its relation to climate changes: inferences from grain-size distributions of a Holocene marine sediment record. Sediment. Geol. 202 (3), 499–508. https://doi.org/10.1016/j.sedgeo.2007.03.015.
Jaccard, S.L., Hayes, C.T., Martínez-García, A., Hodell, D.A., Anderson, R.F., Sigman, D.M., Haug, G.H., 2013. Two modes of change in Southern Ocean productivity over the past million years. Science 339 (6126), 1419–1423. https://doi.org/10.1126/science.1227545.
Kanfoush, S.L., Hodell, D.A., Charles, C.D., Janecek, T.R., Rack, F.R., 2002. Comparison of ice-rafted debris and physical properties in ODP Site 1094 (South Atlantic) with the Vostok ice core over the last four climatic cycles. Palaeogeogr. Palaeoclimatol. Palaeoecol. 182 (3), 329–349. https://doi.org/10.1016/S0031-0182(01)00502-8.
Kohfeld, K.E., Graham, R.M., de Boer, A.M., Sime, L.C., Wolff, E.W., Le Quéré, C., Bopp, L., 2013. Southern Hemisphere westerly wind changes during the Last Glacial Maximum: paleo-data synthesis. Quat. Sci. Rev. 68, 76–95. https://doi.org/10.1016/j.quascirev.2013.01.017.
Kuhn, G., Diekmann, B., 2002. Late Quaternary variability of ocean circulation in the southeastern South Atlantic inferred from the terrigenous sediment record of a drift deposit in the southern Cape Basin (ODP Site 1089). Palaeogeogr. Palaeoclimatol. Palaeoecol. 182 (3), 287–303. https://doi.org/10.1016/S0031-0182(01)00500-4.
Lambert, F., Bigler, M., Steffensen, J.P., Hutterli, M., Fischer, H., 2012. Centennial mineral dust variability in high-resolution ice core data from Dome C, Antarctica. Clim. Past 8 (2), 609–623. https://doi.org/10.5194/cp-8-609-2012.
Lambert, F., Delmonte, B., Petit, J.R., Bigler, M., Kaufmann, P.R., Hutterli, M.A., Stocker, T.F., Ruth, U., Steffensen, J.P., Maggi, V., 2008. Dust-climate couplings over the past 800,000 years from the EPICA Dome C ice core. Nature 452 (7187), 616–619. https://doi.org/10.1038/nature06763.
Lamy, F., Arz, H.W., Kilian, R., Lange, C.B., Lembke-Jene, L., Wengler, M., Kaiser, J., Baeza-Urrea, O., Hall, I.R., Harada, N., Tiedemann, R., 2015. Glacial reduction and millennial-scale variations in Drake Passage throughflow. Proc. Natl. Acad. Sci. Unit. States Am. 112 (44), 13496–13501. https://doi.org/10.1073/pnas.1509203112.
Lamy, F., Chiang, J.C.H., Martínez-Méndez, G., Thierens, M., Arz, H.W., Bosmans, J., Hebbeln, D., Lambert, F., Lembke-Jene, L., Stuut, J.-B., 2019. Precession modulation of the South Pacific westerly wind belt over the past million years. Proc. Natl. Acad. Sci. Unit. States Am., 201905847 https://doi.org/10.1073/pnas.1905847116.
Lamy, F., Gersonde, R., Winckler, G., Esper, O., Jaeschke, A., Kuhn, G., Ullermann, J., Martinez-Garcia, A., Lambert, F., Kilian, R., 2014. Increased dust deposition in the pacific Southern Ocean during glacial periods. Science 343 (6169), 403–407. https://doi.org/10.1126/science.1245424.
Li, F., Ginoux, P., Ramaswamy, V., 2008. Distribution, transport, and deposition of mineral dust in the Southern Ocean and Antarctica: contribution of major sources. J. Geophys. Res.: Atmosphere 113 (D10). https://doi.org/10.1029/2007jd009190.
Li, F., Ginoux, P., Ramaswamy, V., 2010. Transport of patagonian dust to Antarctica. J. Geophys. Res.: Atmosphere 115 (D18). https://doi.org/10.1029/2009jd012356.
Lüthi, D., Le Floch, M., Bereiter, B., Blunier, T., Barnola, J.-M., Siegenthaler, U., Raynaud, D., Jouzel, J., Fischer, H., Kawamura, K., Stocker, T.F., 2008. High-resolution carbon dioxide concentration record 650,000–800,000 years before present. Nature 453 (7193), 379–382. https://doi.org/10.1038/nature06949.
Markle, B.R., Steig, E.J., Roe, G.H., Winckler, G., McConnell, J.R., 2018. Concomitant variability in high-latitude aerosols, water isotopes and the hydrologic cycle. Nat. Geosci. 11 (11), 853–859. https://doi.org/10.1038/s41561-018-0210-9.
Marticorena, B., 2014. Dust production mechanisms. In: Knippertz, P., Stuut, J.B.W. (Eds.), Mineral Dust, A Key Player in the Earth System. Springer Science+-Business Media, Dordrecht, pp. 93–120. https://doi.org/10.1007/978-94-017-8978-3.
Martin, J.H., 1990. Glacial-interglacial CO2 change: the iron hypothesis. Paleoceanography 5 (1), 1–13. https://doi.org/10.1029/PA005i001p00001.
Martínez-García, A., Rosell-Mele, A., Geibert, W., Gersonde, R., Masque, P., Gaspari, V., Barbante, C., 2009. Links between iron supply, marine productivity, sea surface temperature, and CO2 over the last 1.1 Ma. Paleoceanography 24. https://doi.org/10.1029/2008pa001657.
Martínez-García, A., Rosell-Melé, A., Jaccard, S.L., Geibert, W., Sigman, D.M., Haug, G.H., 2011. Southern Ocean dust–climate coupling over the past four million years. Nature 476, 312. https://doi.org/10.1038/nature10310.
Martínez-García, A., Sigman, D.M., Ren, H., Anderson, R.F., Straub, M., Hodell, D.A., Jaccard, S.L., Eglinton, T.I., Haug, G.H., 2014. Iron fertilization of the subantarctic Ocean during the last ice age. Science 343 (6177), 1347–1350. https://doi.org/10.1126/science.1246848.
McCave, I.N., Crowhurst, S.J., Kuhn, G., Hillenbrand, C.D., Meredith, M.P., 2014. Minimal change in Antarctic Circumpolar Current flow speed between the last glacial and Holocene. Nat. Geosci. 7, 113. https://www.nature.com/articles/ngeo2037#supplementary-information.
McCave, I.N., Manighetti, B., Robinson, S.G., 1995. Sortable silt and fine sediment size composition slicing - parameters for paleocurrent speed and paleoceanography. Paleoceanography 10 (3), 593–610. https://doi.org/10.1029/94PA03039.
Neff, P.D., Bertler, N.A.N., 2015. Trajectory modeling of modern dust transport to the Southern Ocean and Antarctica. J. Geophys. Res.: Atmosphere 120 (18), 9303–9322. https://doi.org/10.1002/2015jd023304.
Noble, T.L., Piotrowski, A.M., Robinson, L.F., McManus, J.F., Hillenbrand, C.-D., Bory, A.J.M., 2012. Greater supply of Patagonian-sourced detritus and transport by the ACC to the Atlantic sector of the Southern Ocean during the last glacial period. Earth Planet Sci. Lett. 317–318, 374–385. https://doi.org/10.1016/j.epsl.2011.10.007.
Orsi, A.H., Whitworth, T., Nowlin, W.D., 1995. On the meridional extent and fronts of the Antarctic Circumpolar Current. Deep Sea Res. Oceanogr. Res. Pap. 42 (5), 641–673. https://doi.org/10.1016/0967-0637(95)00021-W.
Paleari, C.I., Delmonte, B., Andò, S., Garzanti, E., Petit, J.R., Maggi, V., 2019. Aeolian dust provenance in central east Antarctica during the Holocene: environmental constraints from single-grain Raman spectroscopy. Geophys. Res. Lett. 46 (16), 9968–9979. https://doi.org/10.1029/2019GL083402.
Petit, J.R., Delmonte, B., 2009. A model for large glacial–interglacial climate-induced changes in dust and sea salt concentrations in deep ice cores (central Antarctica): palaeoclimatic implications and prospects for refining ice core chronologies. Tellus B 61 (5), 768–790. https://doi.org/10.1111/j.1600-0889.2009.00437.x.
Petschick, R., Kuhn, G., Gingele, F., 1996. Clay mineral distribution in surface sediments of the South Atlantic: sources, transport, and relation to oceanography. Mar. Geol. 130 (3), 203–229. https://doi.org/10.1016/0025-3227(95)00148-4.
Revel-Rolland, M., De Deckker, P., Delmonte, B., Hesse, P.P., Magee, J.W., Basile-Doelsch, I., Grousset, F., Bosch, D., 2006. Eastern Australia: a possible source of dust in East Antarctica interglacial ice. Earth Planet Sci. Lett. 249 (1), 1–13. https://doi.org/10.1016/j.epsl.2006.06.028.
Ryder, C.L., Highwood, E.J., Lai, T.M., Sodemann, H., Marsham, J.H., 2013. Impact of atmospheric transport on the evolution of microphysical and optical properties of Saharan dust. Geophys. Res. Lett. 40 (10), 2433–2438. https://doi.org/10.1002/grl.50482.
Ryder, C.L., Highwood, E.J., Walser, A., Seibert, P., Philipp, A., Weinzierl, B., 2019. Coarse and giant particles are ubiquitous in Saharan dust export regions and are radiatively significant over the Sahara. Atmos. Chem. Phys. 19 (24), 15353–15376. https://doi.org/10.5194/acp-19-15353-2019.
Schlitzer, R., 2018. Ocean Data View. https://odv.awi.de.
Shoenfelt, E.M., Winckler, G., Lamy, F., Anderson, R.F., Bostick, B.C., 2018. Highly bioavailable dust-borne iron delivered to the Southern Ocean during glacial periods. Proc. Natl. Acad. Sci. Unit. States Am. 115 (44), 11180–11185. https://doi.org/10.1073/pnas.1809755115.
Starr, A., Hall, I.R., Barker, S., Rackow, T., Zhang, X., Hemming, S.R., van der Lubbe, H.J.L., Knorr, G., Berke, M.A., Bigg, G.R., Cartagena-Sierra, A., Jiménez-Espejo, F.J., Gong, X., Gruetzner, J., Lathika, N., LeVay, L.J., Robinson, R.S., Ziegler, M., Brentegani, L., Caley, T., Charles, C.D., Coenen, J.J., Crespin, J.G., Franzese, A.M., Han, X., Hines, S.K.V., Jimenez Espejo, F.J., Just, J., Koutsodendris, A., Kubota, K., Norris, R.D., dos Santos, T.P., Rolison, J.M., Simon, M.H., Tangunan, D., van der Lubbe, H.J.L., Yamane, M., Zhang, H., 2021.

Antarctic icebergs reorganize ocean circulation during Pleistocene glacials. Nature 589 (7841), 236–241. https://doi.org/10.1038/s41586-020-03094-7.
Struve, T., Pahnke, K., Lamy, F., Wengler, M., Böning, P., Winckler, G., 2020. A circumpolar dust conveyor in the glacial Southern Ocean. Nat. Commun. 11 (1), 5655. https://doi.org/10.1038/s41467-020-18858-y.
Stuut, J.B., Zabel, M., Ratmeyer, V., Helmke, P., Schefuss, E., Lavik, G., Schneider, R., 2005. Provenance of present-day eolian dust collected off NW Africa. Journal of Geophysical Research-Atmospheres 110. https://doi.org/10.1029/2004JD005161. D04202.
Sugden, D.E., McCulloch, R.D., Bory, A.J.M., Hein, A.S., 2009. Influence of Patagonian glaciers on Antarctic dust deposition during the last glacial period. Nat. Geosci. 2, 281. https://doi.org/10.1038/ngeo474.
Thöle, L.M., Amsler, H.E., Moretti, S., Auderset, A., Gilgannon, J., Lippold, J., Vogel, H., Crosta, X., Mazaud, A., Michel, E., Martínez-García, A., Jaccard, S.L., 2019. Glacial-interglacial dust and export production records from the Southern Indian Ocean. Earth Planet Sci. Lett. 525, 115716. https://doi.org/10.1016/j.epsl.2019.115716.
Twohy, C.H., Kreidenweis, S.M., Eidhammer, T., Browell, E.V., Heymsfield, A.J., Bansemer, A.R., Anderson, B.E., Chen, G., Ismail, S., DeMott, P.J., Van Den Heever, S.C., 2009. Saharan dust particles nucleate droplets in eastern Atlantic clouds. Geophys. Res. Lett. 36 (1) https://doi.org/10.1029/2008GL035846.
Újvári, G., Kok, J.F., Varga, G., Kovács, J., 2016. The physics of wind-blown loess: implications for grain size proxy interpretations in Quaternary paleoclimate studies. Earth Sci. Rev. 154, 247–278. https://doi.org/10.1016/j.earscirev.2016.01.006.
Ullermann, J., Lamy, F., Ninnemann, U., Lembke-Jene, L., Gersonde, R., Tiedemann, R., 2016. Pacific-atlantic circumpolar deep water coupling during the last 500 ka. Paleoceanography 31 (6), 639–650. https://doi.org/10.1002/2016pa002932.
Van der Does, M., Brummer, G.-J.A., Van Crimpen, F.C.J., Korte, L.F., Mahowald, N.M., Merkel, U., Yu, H., Zuidema, P., Stuut, J.-B.W., 2020. Tropical rains controlling deposition of saharan dust across the north atlantic ocean. Geophys. Res. Lett. 47 (5), e2019GL086867 https://doi.org/10.1029/2019GL086867.
Van der Does, M., Knippertz, P., Zschenderlein, P., Giles Harrison, R., Stuut, J.-B.W., 2018. The mysterious long-range transport of giant mineral dust particles. Science Advances 4 (12), eaau2768. https://doi.org/10.1126/sciadv.aau2768.
Van der Does, M., Korte, L.F., Munday, C.I., Brummer, G.J.A., Stuut, J.B.W., 2016. Particle size traces modern Saharan dust transport and deposition across the equatorial North Atlantic. Atmos. Chem. Phys. 16 (21), 13697–13710. https://doi.org/10.5194/acp-16-13697-2016.
Veres, D., Bazin, L., Landais, A., Toyé Mahamadou Kele, H., Lemieux-Dudon, B., Parrenin, F., Martinerie, P., Blayo, E., Blunier, T., Capron, E., Chappellaz, J., Rasmussen, S.O., Severi, M., Svensson, A., Vinther, B., Wolff, E.W., 2013. The Antarctic ice core chronology (AICC2012): an optimized multi-parameter and multi-site dating approach for the last 120 thousand years. Clim. Past 9 (4), 1733–1748. https://doi.org/10.5194/cp-9-1733-2013.
Villanueva, J., Grimalt, J.O., Cortijo, E., Vidal, L., Labeyriez, L., 1997. A biomarker approach to the organic matter deposited in the North Atlantic during the last climatic cycle. Geochem. Cosmochim. Acta 61 (21), 4633–4646. https://doi.org/10.1016/S0016-7037(97)83123-7.
Wegner, A., Fischer, H., Delmonte, B., Petit, J.-R., Erhardt, T., Ruth, U., Svensson, A., Vinther, B., Miller, H., 2015. The role of seasonality of mineral dust concentration and size on glacial/interglacial dust changes in the EPICA Dronning Maud Land ice core. J. Geophys. Res.: Atmosphere 120 (19), 9916–9931. https://doi.org/10.1002/2015jd023608.
Wengler, M., Lamy, F., Struve, T., Borunda, A., Böning, P., Geibert, W., Kuhn, G., Pahnke, K., Roberts, J., Tiedemann, R., Winckler, G., 2019. A geochemical approach to reconstruct modern dust fluxes and sources to the South Pacific. Geochem. Cosmochim. Acta 264, 205–223. https://doi.org/10.1016/j.gca.2019.08.024.
Wu, S., Kuhn, G., Diekmann, B., Lembke-Jene, L., Tiedemann, R., Zheng, X., Ehrhardt, S., Arz, H.W., Lamy, F., 2019. Surface sediment characteristics related to provenance and ocean circulation in the Drake Passage sector of the Southern Ocean. Deep Sea Res. Oceanogr. Res. Pap. 103135. https://doi.org/10.1016/j.dsr.2019.103135.
Wu, Y., Roberts, A.P., Grant, K.M., Heslop, D., Pillans, B.J., Zhao, X., Rohling, E.J., Ronge, T.A., Ma, M., Hesse, P.P., Palmer, A.S., 2021. Climatically modulated dust inputs from New Zealand to the Southwest Pacific sector of the Southern Ocean over the last 410 kyr. Paleoceanography and Paleoclimatology, e2020PA003949. https://doi.org/10.1029/2020PA003949.